Creep-Fatigue Behavior of Microelectronic Solder Joints

R.G. Ross, Jr, L.C. Wen, G.R. Mon, E. Jetter and J. Winslow

Jet Propulsion Laboratory, California Institute of Technology, Pasadena, California

ABSTRACT

Even at room temperature, solder joints exhibit both creep and fatigue behavior that is strongly dependent on solder joint configuration, the thermal environment, and the solder alloy properties. The microstructures of solder joints with up to 25 years of aging have been studied using SEM/EDS and metallographic techniques. Data are presented on grain growth and metallurgical composition versus aging time. A special nonlinear finite element creep-fatigue simulation model has been developed, based on measured strain-rate hardness relationships, and used to analytically predict the effects of observed metallurgical changes and the effects of lead stiffness in solder joint creep-fatigue interaction. To corroborate the analytical results, a special bimetallic test fixture has been developed to accelerate the thermo-mechanical loading of solder joints in thermal cycling environments. Measured time-to-failure data for various electronic-package lead configurations/stiffnesses, including gullwing and J-lead, are presented and shown to be in reasonable agreement with the analytical results.

INTRODUCTION

For most microelectronic applications it is not a single high stress event that breaks a component solder joint; rather it is repeated load applications that result in fatigue failure of the solder. Figure 1 presents representative fatigue-life data for 63-37 Sn-Pb solder taken from IBM test results [1]. The plot illustrates the typical dependency between cycles-to-failure and the level of total plastic strain introduced into the solder (total peak-to-peak strain range per cycle). In most microelectronic packages, the principal strain in solder joints is caused by differential expansion between the part and its mounting environment due to changes in temperature (thermal cycles) and/or due to temperature gradients between the part and the board.

The function of strain relief elements—such as the flexible metal leads of the electronic components—is to lower the differential-expansion induced loads (stresses) on the solder joints to levels below the solder yield strength, thus minimizing the generation of plastic strain. Unfortunately, under typical multi-hour loading conditions the solder joints can still be expected to undergo modest levels of strain due to creep of the solder in response to the applied elastic forces from the strain relief elements. This creep-induced strain has the same damaging effect as more immediately induced plastic strain, and must be summed with the plastic strain to achieve the total strain that is correlated with fatigue life in Fig. 1.

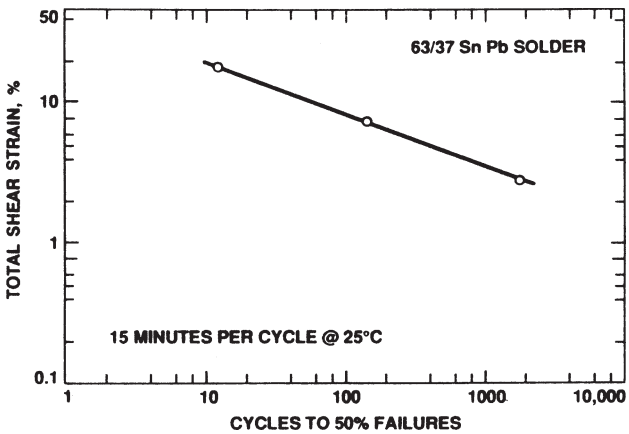

Figure 1. Solder-joint fatigue life versus cyclic strain level at 25°C (IBM data [1]).

Because of creep effects, the total strain range during any given loading cycle can be a strong function of solder temperature, the loading time per cycle, the applied solder stress, the spring constant of the strain relief elements, and the chemical

Materials Research Society Symposium Proceedings
Mechanical Behavior of Materials and Structures in Microelectronics
1991 MRS Spring Meeting, Anaheim CA, April 30 - May 4, 1991

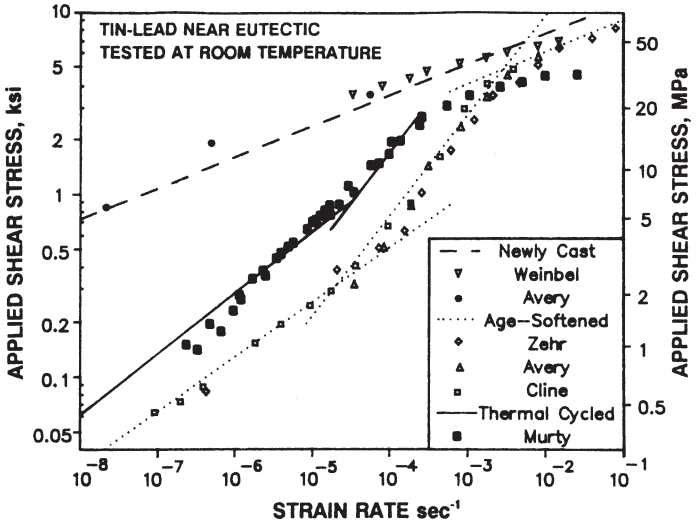

Figure 2. Strain rate versus stress for 63-37 Sn-Pb solder at room temperature.

composition and size of the solder grains. Figure 2 illustrates the strong sensitivity of solder strain rate (creep rate) to the solder stress resulting from the load applied by the electronic part/board system (including elastic strain relief elements) during the loading cycle [2-6]; also included is the sensitivity to the heat treatment condition of the solder. Upon examination, it is apparent that Fig. 2 describes both plastic strain and creep strain as a continuum, with plastic strain associated with the high strain rate (right-hand) end of the plot, and creep strain associated with the remainder of the plot. Although Fig. 2 is for room-temperature solder, the strain (creep) rate for a given applied stress can be extrapolated to other temperatures by noting that creep rate increases by a factor of approximately 1.8 for each 10°C increase in temperature [7]. Figure 2 is useful for assessing the rough magnitude of creep effects likely to be encountered in any given solder loading application. The implication of these data is that creep related strain—and in particular the time, temperature, and elastic-stiffness dependency of creep—must be carefully factored into the design and testing of solder joints and component mounting techniques over a very broad range of cyclic frequencies.

The objective of the ongoing study described here is to understand the range of metallurgical conditions likely to be encountered in typical spacecraft solder joint applications, and to develop quantitative insights into the role of key parameters such as metallurgical conditions and component lead flexibility in determining the creep-fatigue durability of solder joints. The study includes a combination of detailed metallurgical examinations of representative solder joints ranging in age up to 25 years, and extensive finite element modeling and thermal-cycle testing of representative solder joints.

SOLDER JOINT METALLURGICAL INVESTIGATIONS

Because spacecraft electronics often range in age from a few months to many years, an important issue is the variability in solder creep-fatigue properties that may exist over the life-cycle of the hardware due to changing metallurgical properties.

In general, freshly solidified solder has a fine grain structure with supersaturated lead-rich regions, and is considerably more resistant to thermal creep than older solder (see Fig. 2). Because the equilibrium concentration of tin and lead in the grains is a strong function of temperature, the chemical composition of the solder grains is determined by the cooling rate during solidification and the aging time following solidification. Over a period of months, the excessive elemental concentrations in the unstable supersaturated regions gradually diffuse out, and the solder becomes age-softened. During this short-term aging, the overall microstructure displays some coarsening, but there is no significant grain growth. With prolonged aging, or exposure to elevated temperature, grain growth is experienced; this can cause the solder to return toward a more creep-resistant condition with reduced fatigue endurance.

To evaluate the properties of solder joints in typical flight electronics, a number of chassis with years of room-temperature aging were acquired from various past and present JPL flight programs. These include Mariner 5 (1967), Mariner MVM (1973), and Viking (1975), as pictured in Fig. 3. In addition, numerous freshly made solder joints with carefully controlled aging parameters were examined. Each sample was cross-sectioned and analyzed by SEM to determine the specimen's metallurgical structure.

Table I. Solder Metallurgical Properties of Cross-sectioned Solder Joints with Various Ages and Thermal Exposure Histories.

Sample Aging History	Grain Size (microns)	Lead-rich Phase		Tin-rich Phase	
		% Pb	% Sn	% Sn	% Pb
Just soldered	1.17	71.2	28.8	80.4	19.6
10 hours @ 150°C	2.97	79.3	20.7	97.9	2.1
6 hours @ 100°C	1.42	83.3	16.7	91.5	8.5
1.5 years @ 23°C	2.08	97.3	2.7	96.9	3.1
15 years @ 23°C (Viking '75)	8.76	97.6	2.4	99.9	0.1
18 years @ 23°C (MVM '73)	9.03	98.3	1.7	100.	0.0
24 years @ 23°C (Mariner '67)	9.56	98.6	1.4	99.7	0.3

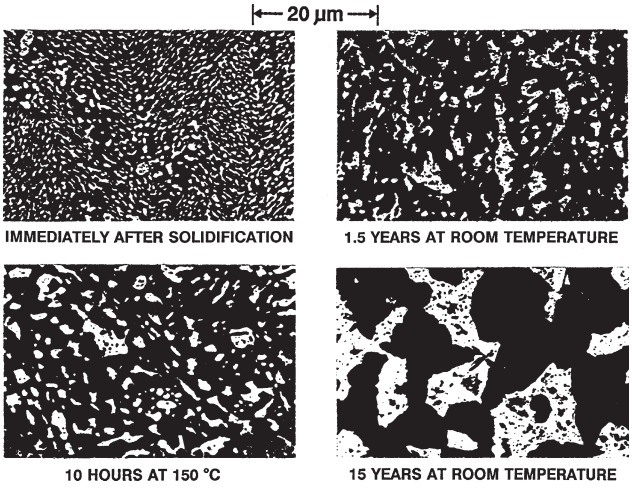

Figure 4. SEM photographs showing cross-sections of solder of various ages (tin is dark region).

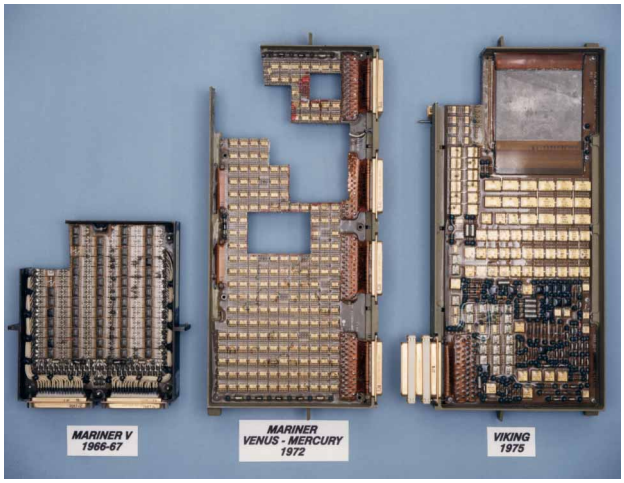

Figure 3. Spacecraft electronics from previous JPL programs used for investigation of properties of aged solder.

Table I displays approximate metallurgical concentration measurements made using SEM-EDS. The increased purity of the grains in the aged solder correlates with that expected from solder's phase diagram. In addition, Fig. 4 graphically illustrates the enormous levels of grain growth found; each of the photographs in this collage is at the same magnification. Note the fine (1 micron) grain of the freshly made solder in contrast to the 10-micron grains of the aged solder.

FINITE ELEMENT CREEP-FATIGUE STRAIN SIMULATION

A two pronged analytical/experimental approach has been undertaken to assess the possible influence of the observed metallurgical variability on solder creep-fatigue, and to determine quantitative estimates of the importance of other solder-joint design features such as strain relief elements.

Because of the relatively long multi-hour temperature cycles associated with spacecraft electronics, creep relaxation of applied stresses can play a major role in the total solder strain experienced over a mission life. For this reason a specialized nonlinear finite-element creep simulation computer program was formulated to directly utilize the stress and metallurgically-dependent creep data of Fig. 2, including the temperature dependence of these data. Because part lead dimensions and flexibility determine the total creep deflection (solder strain range), these parameters were carefully preserved in elastic beam elements used to model each part lead. To provide insight into the solder creep process, the solder itself was subdivided into separate vertical-tension-compression and horizontal-shear creep elements distributed along the solder fillet. A typical computer run consists of several thousand time-step solutions displaying the progressive total plastic/creep strain developed in each solder element during a multi-thermal-cycle exposure.

Figure 5 displays the computed strain response to accelerated temperature cycling for typical gullwing flat-pak packages as a function of vertical lead height as defined in Fig. 6. The data correspond to the -25°C to 100°C temperature cycle shown in the center of Fig. 5, combined with the expansion properties of the accelerated test fixture used in JPL's solder joint testing program; this produces a horizontal

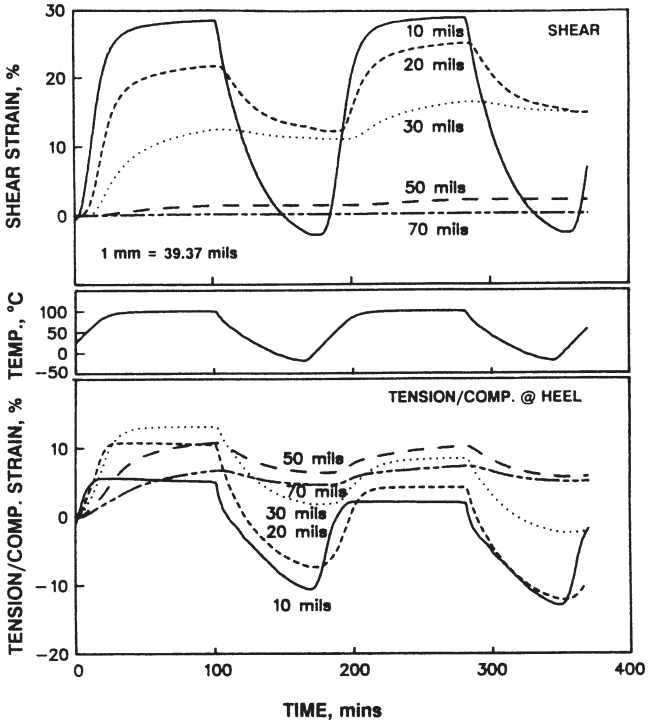

Figure 5. Solder cyclic strain range response to temperature cycling for gullwing flat-paks with various vertical lead bend heights.

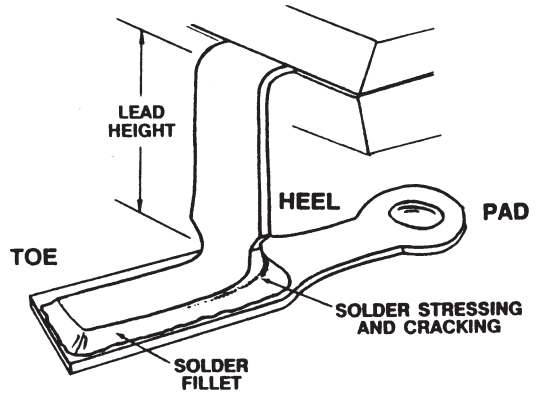

Figure 6. Gullwing solder joint nomenclature.

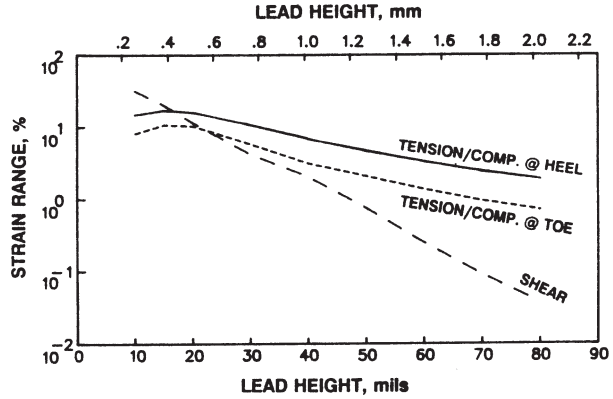

Figure 7. Dependence of strain cycling range on flat-pak lead height for -25°C to 100°C thermal cycle with ±1.2 mil lead deflection.

deflection of the top of the part lead relative to the circuit board of ±1.2 mils (0.03 mm). The top curves in Fig. 5 depict the solder horizontal shear strain resulting from this accelerated temperature cycling, while the bottom diagram depicts the corresponding vertical tension-compression strain at the solder-joint heel. Note the significant reduction in total strain range associated with higher, more flexible leads, and the tendency for the solder strain to include both a cyclic fatigue component together with a progressive creep-rupture drift. The computed strain-range dependence on lead height is summarized in Fig. 7 and suggests that shear failure should dominate with short lead heights, and tension-compression failure at the heel should dominate with high lead heights.

Figure 8 plots computed strain range versus lead height for three solder heat treatments: freshly cast, thermal cycled, and aged. These conditions correspond to the three data sets displayed in Fig. 2. For the same gullwing lead height, aged solder suffers the largest strain range, and freshly-cast solder the smallest. Figure 9 summarizes the computed strain ranges for four lead types and three solder heat treatments.

Finally, Fig. 10 presents the frequency dependence of strain-range for typical J-lead packages subjected to 81°C isothermal mechanical cycling with a fixed ±0.7 mil (0.18 mm) deflection. At high frequency—where there is little dwell time to permit creep relaxation—the shear and toe strain ranges are quite low. At low frequencies, the solder strain range is greater due to creep, and the

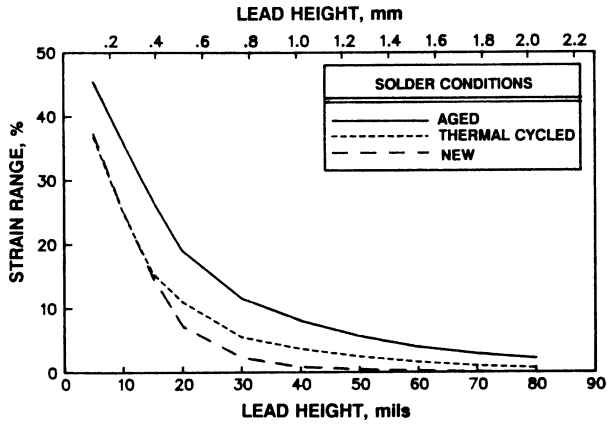

Figure 8. Effect of solder aging condition on flat-pak solder strain range for -25°C to 100°C thermal cycle with ±1.2 mil lead deflection.

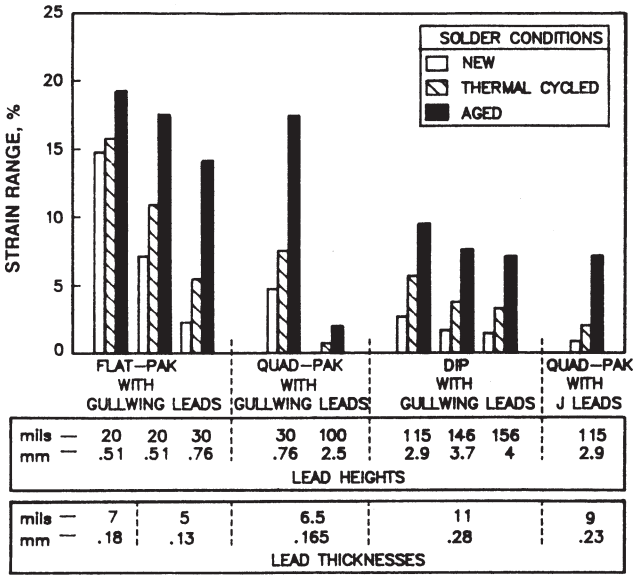

Figure 9. Comparison of computed strain range with various lead types and solder aging conditions for -25°C to 100°C thermal cycles with ±1.2 mil lead deflection.

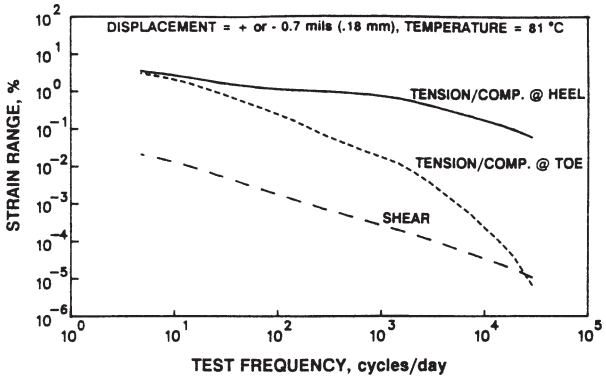

Figure 10. Effect of cyclic frequency on computed strain range for J-lead parts at 81°C.

likelihood of failure is enhanced. The normal heel strains decrease with increasing test frequency at a rate of about one decade of strain range for every two decades of test frequency — considerably less than the changes in toe and shear stresses with changing test frequency.

SOLDER JOINT TESTING PROGRAM

A necessary element of verifying the solder fatigue models and metallurgical investigations and reducing them to applicable design recommendations is conducting a number of carefully controlled tests. To this end a special bimetallic test board (Fig. 11) was developed to conduct accelerated thermal-cycle fatigue tests on a variety of electronic component package styles. A key advantage of the bimetal fixture, in addition to the high acceleration ratio, is the fact that it can be directly placed into the SEM for nondestructive microscopic examination of solder joint health before, during, and after thermal cycling. Figure 12 illustrates a typical failure of a gullwing flat-pak with a short 10-mil (0.25mm) lead bend height. SEM analysis as well as 10X-50X optical microscopy was used extensively to quantify damage level as a function of number of temperature cycles; testing for intermittent electrical opens was found to be much less effective and was abandoned after initial trials.

Figure 13 compares degradation rates for various package styles and lead heights for the same -25°C to 100°C thermal cycle (2.4 mil deflection range) used in the analytical simulations. The data reflect the most degraded solder joints on each package — usually the corner joints, which suffer simultaneous strains in two directions.

Figure 14 contrasts the experimentally determined fatigue endurance of flat-pak packages with

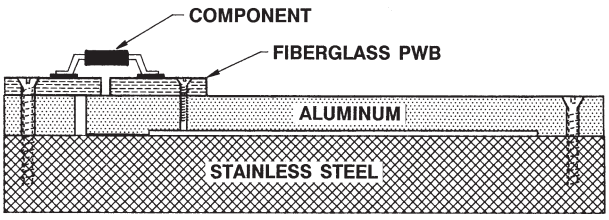

Figure 11. JPL bimetallic test board for accelerated thermal-cycle testing.

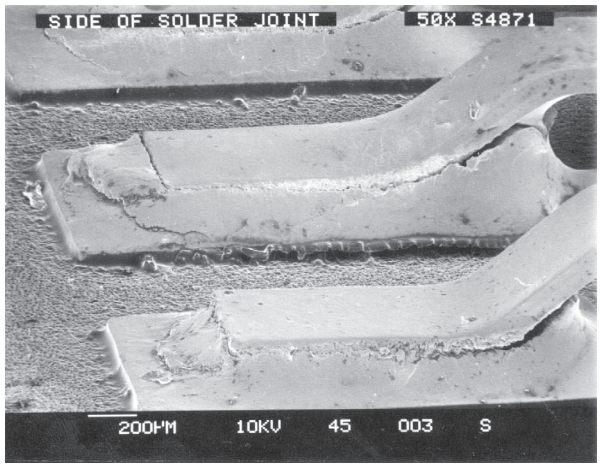

Figure 12. Typical heel-to-toe crack propagation for gull-wing solder joints.

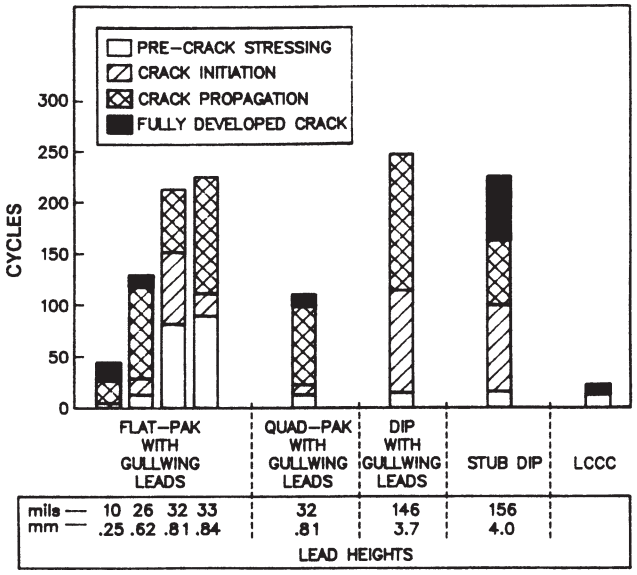

Figure 13. Summary of solder joint degradation for various package/lead configurations with bimetallic test fixture (-25°C to 100°C cycle).

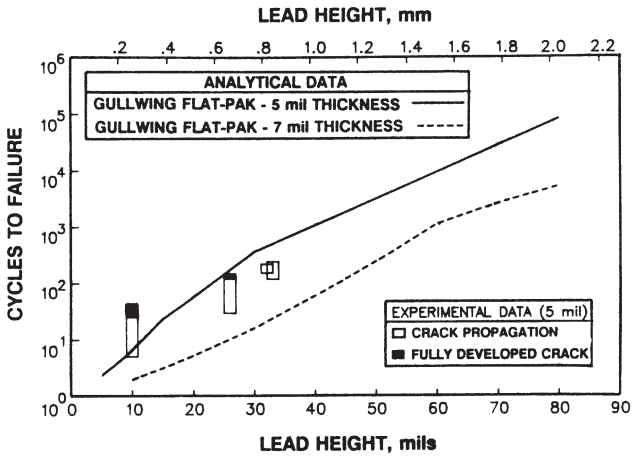

Figure 14. Comparison of analytical and measured dependence of solder joint fatigue life versus flat-pak lead bend height.

the analytical results presented earlier in Fig. 9 for the same conditions. For this comparison the strain range ordinate in Fig. 9 was translated to cycles-to-failure through the use of the Coffin-Manson fatigue data displayed in Fig. 1; the experimental points displayed are determined from Fig. 13. The agreement is considered to be reasonably good.

ACKNOWLEDGMENT

The work described in this paper was carried out by the Jet Propulsion Laboratory, California Institute of Technology, under contract with the National Aeronautics and Space Administration.

REFERENCES

1. Wild, R.N., *Some Fatigue Properties of Solders and Solder Joints*, IBM Report No. 7AZ000481, IBM Federal Systems Division, New York, 1975.

2. Avery, D.H. and Backofen, W.A., "A Structural Basis for Superplasticity," *Transactions of the ASM*, v.58, 1965, pp. 551-562.

3. Cline, H.E. and Alder, T.H., "Rate Sensitive Deformation in Tin-Lead Alloy", *Trans. AIME*, v.239, 1967, pp. 710-714.

4. Weinbel, R.C., Tien, J.K., Pollak, R.A., and Kang, S.K., "Creep-Fatigue Interaction in Eutectic Lead-Tin Solder Alloy", *J. of Material Science Letter*, v.6, 1987, pp. 3091-3096.

5. Zehr, S.W. and Backofen, W.A., "Superplasticity in Lead-Tin Alloys", *Transaction of the ASM*, v.61, 1968, pp. 300-312.

6. Murty, G.S., "Stress Relaxation in Superplastic Materials", *J. of Material Science*, v.8, 1973, pp. 611-614.

7. Kashyap, B.P. and Murty, G.S., "Experimental Constitutive Relations for the High Temperature Deformation of a Pb-Sn Eutectic Alloy", *Materials Science and Engrg*, v.50, 1981, pp. 205-213.